Flexor digitorum brevis utilises elastic strain energy to contribute to both work generation and energy absorption at the foot

Ross E. Smith[1], Glen A. Lichtwark[1], Luke A. Kelly[1,*]

[1]School of Human Movement and Nutrition Sciences, The University of Queensland, Brisbane, Australia.

Intrinsic foot muscles, foot biomechanics, muscle dynamics, foot energetics

*Contact corresponding author at: l.kelly3@uq.edu.au

Summary Statement

This paper demonstrates an adaptive mechanism for the intrinsic foot muscles to make versatile contributions to whole-body accelerations and decelerations.

Abstract

The central nervous system utilizes tendon compliance of the intrinsic foot muscles to aid the foot's arch spring, storing and returning energy in its tendinous tissues. Recently, the intrinsic foot muscles have been shown to adapt their energetic contributions during a variety of locomotor tasks to fulfil centre of mass work demands. However, the mechanism by which the small intrinsic foot muscles are able to make versatile energetic contributions remains unknown. Therefore, we examined the muscle-tendon dynamics of the flexor digitorum brevis during stepping, jumping, and landing tasks to see whether the central nervous system regulated muscle activation magnitude and timing to enable energy storage and return to enhance energetic contributions. During step ups and jumps, energy was stored in the tendinous tissue during arch compression, and during arch recoil, the fascicles shortened at a slower rate than the tendinous tissues while the foot generated energy. During step downs and landings, the tendinous tissues elongated more and at greater rates than the fascicles during arch compression while the foot absorbed energy. These results indicate the central nervous system utilizes arch compression to store elastic energy in the tendinous tissues of the intrinsic foot muscles to add or remove mechanical energy when the body accelerates or decelerates. This study provides an adaptive mechanism used to enable the foot's energetic versatility and further indicates the value of tendon compliance in distal lower limb muscle tendon units in locomotion.

Introduction

The human foot is known to possess spring-like compliance in its long arch, which allows energy savings and aids in propulsion during locomotion (Ker et al., 1987; Stearne et al., 2016). The plantar aponeurosis, a thick, ligamentous connective tissue sheath along the foot's plantar surface, makes passive contributions to the foot's arch-spring by absorbing and returning energy over the course of gait stance (McDonald et al., 2016; Welte et al., 2021). The intrinsic foot muscles also span the length of the long arch and have also been suggested to contribute to the foot's arch-spring mechanism (Kelly et al., 2019). Additionally, the intrinsic foot muscles actively modulate the foot's mechanics to meet energetic requirements during tasks requiring rapid accelerations and decelerations (Smith et al., 2021). Therefore, the intrinsic foot muscles (IFM) are thought to enable the foot's functional versatility during a range of locomotive modalities.

To accelerate or decelerate our body during locomotion, muscles act to generate or dissipate mechanical energy. The ankle plantar flexors are the largest average power contributors to walking and running (Farris and Sawicki, 2012), and a substantial amount of the power contributed is by the elastic tendinous tissue (Lichtwark and Wilson, 2006). This is possible due to the interaction between the short-pennate muscle fibres of the gastrocnemii and soleus and the Achilles tendon. For example, the first half of stance phase in locomotion, dorsiflexion of the ankle joint results in elongation of the muscle-tendon unit (MTU), while the fascicles of the plantar flexors remain quasi-isometric, facilitating stretch of the elastic tendon (Fukunaga et al., 2001; Lichtwark and Wilson, 2006; Lichtwark et al., 2007). Throughout this period, neural drive to the ankle plantar flexors is controlled so that force produced by the muscles is sufficient to maintain a quasi-isometric contraction, allowing strain energy to be stored in the stretching tendon. During propulsion, the energy stored in the tendon is returned to the body via tendon recoil delivering mechanical power to propel the body forward (Fukunaga et al., 2001; Lichtwark et al., 2007).

Decoupling the MTU and tendon length changes from the contractile length change also enables stored energy to be returned through MTU recoil while the fascicles actively shorten, allowing supramaximal power outputs from the ankle plantar flexors when generating energy during accelerations (Kurokawa et al., 2003; Farris et al., 2016, Wade et al., 2018). However, energy storage prior to enhanced energy generation is performed by muscular work through fascicle shortening, such that the energy stored in the Achilles during ankle dorsiflexion is subsequently returned by the tendon at a greater velocity than of its fascicles during propulsion, acting to "amplify" plantar flexor power outputs (Roberts and Azizi, 2011). When decelerating the body, the ankle plantar flexor's MTU lengthen significantly more than the fascicles, acting as a velocity buffer from high-power inputs into muscles (Werkhausen et al., 2017). For this to occur, the initial high-velocity elongation of the MTU is largely attributed to tendon elongation, rather than actively lengthening muscle fibres. Subsequently, as force and velocity decline, the tendon recoils and the muscle fibres actively lengthen to dissipate the energy that is stored in the stretched tendon. This

mechanism delays and extends the period over which the muscle dissipates energy, potentially protecting from excessively high strains and forces in the muscle tissue (Werkhausen et al., 2017). Therefore, the architectural arrangement of muscles with short fibres and a long compliant tendon at the ankle joint enables functional versatility required beyond steady state locomotion.

In a series of recent experiments, we have shown that during stepping, jumping, and landing, the central nervous system adapts the energetic behaviour of the foot to perform net work based on centre of mass (COM) work demands (Riddick et al., 2019; Smith et al., 2021). In these experiments, 8-17% of the mechanical work performed at the COM is contributed by structures within the foot. We have also shown that if we remove active force production within the foot by anaesthetizing the IFM, the energetic contributions of the foot to COM work decrease by ~3% during running, jumping and landing (Farris et al., 2019; Smith et al., 2021). These findings indicate that the IFM are directly linked to the foot's functional versatility and capacity to dissipate and generate mechanical energy. However, the mechanisms for dissipating or generating significant amounts of energy when the IFM (e.g. flexor digitorum brevis (FDB) or abductor hallucis (AH)) possess relatively short muscle fibres is currently unknown. A recent study has demonstrated that the FDB facilitates elastic storage and return in its tendonous tissues during cyclical tasks designed to emulate the loading demands of steady state locomotion (Kelly et al., 2019). Therefore, it is possible that IFM may utilize their elastic elements to enhance energy generation and dissipation capacities within the foot, however this has yet to be explored.

Here we examined the dynamic behaviour of the FDB MTU and muscle fascicles during tasks where mechanical energy was generated and dissipated at the foot. We hypothesized that FDB muscle-tendon behaviours and activity will display specific behaviours based on the energetic function of the foot and by the intensity of the task (increased foot power generation or absorption) such that: 1) during foot energy generation, the FBD fascicles would have reduced lengthening magnitude and velocity relative to the MTU during initial loading of the foot (suggesting energy storage in FDB tendinous tissue) and would actively shorten during propulsion, but with lower velocities than the MTU (suggesting energy release from FDB tendinous tissue) and that this effect will be greater with task intensity; 2) and during foot energy dissipation, FBD muscle fascicles would lengthen with lower magnitudes and velocities than the MTU (suggesting that energy is storage in FDB tendinous tissue) and that this effect will be greater with task intensity.

Methods

Participants

14 (12 male, 2 female, 26.2 ± 14.8 years, 1.72 ± 0.23 m, 73.9 ± 15.9 kg) participants were recruited in accordance with an a-priori analysis (G-power, version 3.1.9.2, Germany) powered at β=0.90 for a large effect of d=1, and α=0.05. One subject's data was excluded as their ultrasound fascicle data

was of too low a quality to measure accurately (n=13 for all analyses). All participants were between 18-45 years old, were recreationally active (able to walk and run for 30 mins consecutively) and had no lower limb injuries within 12 months of data acquisition. The University of Queensland's Human Research Ethics Committee approved this research protocol and ensured it operated in accordance with the Declaration of Helsinki. Written informed consent was obtained from all participants.

Experimental task

Participants performed two energy generation tasks (step up or jump) and two energy dissipation tasks (step down or landing). All tasks were performed unilaterally to ensure no compensatory efforts from the non-studied limb. The energy generation tasks involved stepping and jumping from a force plate on the ground onto a 20.5 cm box located in front of the participants. A piece of tape was placed 1 cm from the edge of the force plate closest to the box. The most distal portion of each participant's foot was aligned with this tape piece before each trial, ensuring similar step or jump distances in fore-aft direction. For the energy dissipation tasks, participants were asked to step down or drop from the same 20.5cm box onto a force plate in front of the box. The box was placed 5 cm from a tape piece on the force plate which was used as a stepping or landing target for the heel. The order of energy generation or dissipation tasks was randomized. Before collection trials both with and without the custom foam shoe (discussed below), participants were allowed familiarisation trials, which were simply practice trials for all tasks. No data was collected and these trials were performed to ensure correct task execution and participant comfort. Following completion of all familiarisation tasks, an ultrasound transducer was secured with cohesive bandage to the plantar surface of their dominant foot, over the muscle belly of the FDB as previously described (Kelly et al. 2019). Foot dominance was determined by asking participants which foot they would kick a ball with. After securing the transducer and ensuring ultrasound image quality, a participant-specific custom foam shoe was secured to the foot to protect the transducer from damage and to maintain reasonably constant contact pressure of the probe against the foot (Fig. 1). After fitting of the shoe, participants then repeated the protocol detailed above. Additional familiarization trials for all tasks were encouraged for all participants after the fitting of the shoe to encourage participant comfortability with task performance.

To perform the step-up trial, participants lifted their non-dominant foot onto the box while pushing off of the force plate with their dominant foot in order to propel themselves onto the box. Participants were cued to make contact with the box on their non-dominant foot only after the dominant foot's heel was off the ground to encourage push-off power generation by the stance foot. During the jumping task, participants jumped from their dominant foot onto the box, landing on both feet to ensure safety. Participants were discouraged from swinging the non-dominant leg to generate energy for upward propulsion of the COM. However, due to balance constraints from the unilateral task, use of the arms and arm swing were permitted.

For the step-down trials, participants stepped down from the box onto their dominant foot, and were cued to limit use of the non-dominant leg to lower the COM. For drop landings, participants dropped from the box onto their dominant foot. A successful landing trial was one where participants leaned anteriorly until they began to fall, then immediately lifted their non-dominant leg off of the box and landed on their dominant foot. This method has been described previously by the cue "walking the plank" (Smith et al., 2021) and was used to discourage lowering of the COM by the non-dominant limb before the drop's initiation.

Custom Foam Shoe

All foam shoes followed the same design but were customised to fit each participant. The shoes were made from two sheets of Shore A45 Ethylene vinyl acetate foam (15mm thickness, MetroFoam, Silverwater, NSW, Australia), glued together with contact adhesive. This foam hardness was chosen to minimize energy absorption / dissipation within the foam, whilst retaining comfort. The bottom sheet (Figure 1.B) was cut to a generic shoe shape and sized to each participant. The top sheet (Figure 1.A1 & A2) was cut as a copy of the bottom with a gap between the heel and forefoot sections to house the ultrasound transducer (Figure 1.C). Incisions were made into the foam to reduce the bending stiffness of the shoe and facilitate natural motion of the arch and metatarsalphalangeal (MTP) joints. Figure 2 depicts the orientation of the probe against the foot's plantar surface in order to obtain a satisfactory ultrasound image.

Data Processing and Analysis

Kinematics and Kinetics

3D-motion capture data was collected for all experimental tasks at 250 Hz (Oqus, Qualisys, Gothenburg, Sweden). To quantify motion of the pelvis and lower limb, reflective markers (9 mm, B&L Engineering, Santa Ana, CA) were placed on the left and right posterior superior iliac crests and anterior superior iliac crests to define the pelvis segment; on the medial and lateral epicondyles to define the thigh segment; and on the medial and lateral malleoli to define the shank segment. Additional 4-marker rigid clusters were secured to the thigh and shank segments to track motion of their respective segments. To establish individual foot segments and track ankle and foot motion during the experimental trials, reflective markers were also placed on the peroneal tubercle, sustentaculum tali, and calcaneal tuberosity to define the calcaneus; on the medial aspect of the first metatarsal base and head, superior aspect of the second metatarsal base and head, and lateral portion of the fifth metatarsal base and head to define the metatarsal segment; and on the medial aspect of the proximal first phalanx, and the superior aspects of the second and fourth intermediate phalanges to establish a toe segment in accordance with previous literature (Leardini et al., 2007; Kelly et al., 2015).

A static calibration trial was captured to establish segment dimensions, and a six-degree of freedom model was constructed for the calculation of joint kinematics and kinetics. Using Visual 3D (C-Motion, Inc., MD, USA), data were low-pass filtered with a second-order bi-directional Butterworth filter at 25 Hz. Joint rotations are expressed about their proximal reference segment. Ankle joint rotation was expressed as rotation of the calcaneus about the shank, while deformation of the longitudinal arch (LA) was quantified as sagittal plane rotation of the metatarsal segment relative to the calcaneus. Rotational polarity of all joints and their Cardan rotational sequences were assigned using a right-hand rule with X as the longitudinal axis, Y is the anteroposterior axis, and Z is the mediolateral axis for tri-planar calculations.

Ground reaction force data was collected at 2500 Hz (AMTI, Watertown, MA, USA) and was also filtered in Visual 3D using the same frequency cut-off to avoid the possibility of sagittal plane moment artefacts (Derrick et al., 2020). Using filtered force data and joint kinematic data, net internal joint moments were calculated using a Newtonian-Euler inverse dynamics solutions within Visual3D software. Relative segment masses, joint centres, COM locations, and moments of inertia were based on previous literature (Dempster, 1955; Hanavan, 1964). Foot power was calculated using a unified deformable (UD) segment analysis that is described in previous literature (Takahashi et al., 2012; Takahashi et al., 2016). The UD segment analysis models the foot as a hybrid segment which includes a rigid, proximal component and a distal, deformable component (Takahashi et al., 2012). It provides as estimate of the power of all structures distal to the calcaneus (i.e. fat pads, plantar ligaments, etc.) and has previously been used to describe the foot's gross energetic function (Riddick et al., 2019; Smith et al., 2021). Foot work was calculated as trapezoidal integration of the UD foot power metric.

For step-up data analyses, time-series data waveforms begin at the first 10% deviation from bodyweight of vertical ground reaction force component, through to take-off. For the jump analyses, time-series data begin at countermovement initiation and continue through to take-off. where countermovement initiation was defined as the point at which pelvis-segment velocity under a -0.075 m/s threshold (Smith et al., 2021). This was chosen in order to account for oscillations in pelvis velocity during unilateral stance. Data used in statistical comparisons were taken from phases in time series data from the point at which FDB MTU lengths began to shorten by more than 0.1 mm for two consecutive frames until take-off (propulsion start). For both step-downs and landings, time-series data were taken from foot contact until pelvis velocity was no longer negative. Data used in statistical comparisons were taken from highlighted phases in time-series data from the point at which FDB MTU lengths were either lengthening until length change ceased to exceed 0.1 mm for five consecutive frames (0.02 s) (deceleration end). For all tasks, time series data is presented as total movement time normalized to 101 points.

Muscle-Tendon Dynamics and Activation

B-mode ultrasound imaging for the flexor digitorum brevis (FDB) was collected using a custom-built T-shaped 128-element, 4cm ultrasound transducer (LZ 7.5/60/128Z-2, Telemed, Vilnius, Lithuania). The transducer was placed over the FDB muscle belly, in line with the second metatarsal and secured with self-adhesive tape (Kelly, 2019). Capture frame-rate ranged from 134-171 Hz and varied based on changes in settings within Telemed software that were made to optimize the image for data analysis. Muscle fascicle data were processed using a semi-automated optic affine flow algorithm to measure the movement of muscle fascicles and apply the observed displacement of the muscle to defined distal and proximal endpoints from frame to frame (Farris and Lichtwark, 2016; Cronin et al., 2011). According to a model used previously (Kelly et al., 2015; Kelly et al., 2019), FDB MTU length data was calculated from kinematic data as the distance between the muscle model's origin at the calcaneus, to its insertion at the phalanges about a tethering point at the MTP joint. Mean fascicle and MTU velocity were calculated as the first derivative of FDB fascicle or MTU length with respect to time. For all tasks, MTU and fascicle velocities that are positive indicate lengthening velocities and negative for shortening velocities.

Muscle activation data (EMG) for the FDB was sampled at 4000 Hz, amplified by x1000, and recorded between a 30-1000 bandwidth (MA300, Motion Lab Systems, Baton Rouge, LA). Fine-wire electrodes (0.051 mm stainless steel, Teflon coated, Chalgren, USA) were inserted into the FDB muscle under ultrasound guidance (10 MHz linear array, SonixTouch, Ultrasonix, BC, Canada) in accordance with previously described methods (Kelly et al., 2012; Kelly et al., 2015; Kelly et al., 2018). The EMG data was processed using a custom Matlab (Mathworks, Nattick, MD, USA) script that; removed any D.C. offset; applied a second-order Butterworth high-pass filter at 50 Hz; rectified the signal; low-pass filtered the signal at 10 Hz for data smoothing; and normalized to the maximum rectified signal amplitude recorded across all tasks. Thus, EMG signals are presented as a percentage of peak activation, where peak activation was the largest activation value across all tasks.

Statistics

A two-way (muscle level x task intensity), within-subjects, repeated measures ANOVAs (Jamovi, version 1.6, www.jamovi.org) were performed for both energy generation and dissipation tasks to assess whether there were differences in MTU and fascicle velocity (muscle level) and whether this was influenced by task velocity constraints (task intensity). Post-hoc multiple comparisons *t*-tests were performed to detect the nature of any interaction effects, and Bonferroni corrections were made to reduce likelihood of type 1 error with multiple comparisons. Additionally, paired-samples t-tests were performed to assess the effect of increased task velocity on peak power and work performed at the foot, as well as mean and peak FDB EMG. Statistical significance for all statistical tests was set at $p \leq 0.05$. All results are reported as mean values ± standard deviation.

Results

Energy Generation

MTU and fascicle behaviour

Figure 3A and B show FDB MTU and fascicle length changes during step ups and jumps. The MTU length changes for both tasks (Step ups ~8 mm; Jumps ~10 mm) were much larger than fascicle length changes (Step ups ~0.9 mm, Jumps ~0.7 mm). We also observed differences in the timing of length changes occurring at the MTU and the fascicles between step ups and jumps. During step ups, the fascicles begin shortening as early as 10% of total movement time and continue shortening until take-off, where the MTU begins shortening at ~60% time. During the jumps, fascicle shortening is preceded by a phase of slight lengthening from ~30-75% total movement time, after which the fascicles shorten until take-off. MTU length changes are larger by an order of magnitude and show a clear period of lengthening from 30-90% total movement time, followed by rapid shortening prior to take-off. During both tasks, FDB fascicle shortening preceded FDB MTU shortening, further highlighting the dissociation in the dynamic behaviour of the contractile and tendinous tissues. FDB MTU and fascicle velocities are shown in Figure 3D and E. We observed main effects for muscle level (MTU vs fascicle, $p < 0.001$) and task intensity (step ups vs jumps, $p < 0.001$), as well as an interaction effect ($p < 0.001$). Post hoc *t*-tests revealed that while mean fascicle shortening velocities were faster during jumps (-9.83 ± 7.6 mm/s) than during step-ups (-3.81 ± 3.1 mm/s, $p = 0.039$), the interaction effect was largely driven by the substantially higher MTU shortening velocities during the jumps (-106.92 ± 36.7 mm/s) compared to the step-ups (-38.6 ± 11.1 mm/s, $p < 0.001$).

Muscle activation

The FDB EMG signals also display differences in the timing of activation between tasks (Figure 3C). During the step-ups, muscle activation increased relatively quickly (19-41% of max) and peaks at ~50% of total movement time and begins to decay at ~75% of total movement time. During the jumps, activation increases from ~35% to peak at ~80% of total movement time, after which it decays. Neither mean (Step ups: 23.2 ± 12.68%; Jumps: 25.3 ± 6.47%, $p = 0.419$) or peak FDB EMG (Step ups: 39.6 ± 20%; Jumps: 44.25 ± 8.79%, $p = 0.375$) were different between step ups and jumps.

Foot energetics

Peak power generation (Step ups = 73.2 ± 38 W, Jumps = 380 ± 133.2 W) and positive work (Step ups = 9.1 ± 4.95 J, Jumps = 20.8 ± 8.47 J) at the foot was greater during jumps, compared to the step-ups (both $p < 0.001$). The primary burst of positive power at foot occurs concurrently with the periods of peak MTU and fascicle shortening velocity (Figure 3F), indicating recoil of the MTU is contributing positive power at the foot.

Energy Dissipation

MTU and fascicle behaviour

FDB MTU and fascicle lengths for step-downs and landings are shown in Figure 4A and B. The MTU undergoes an initial lengthening after foot contact, followed by a plateau (dissipation end) during both step down (33% of total movement time) and landing (48% of total movement time) tasks. The FDB fascicles lengthen slightly, but generally function quasi-isometrically during both tasks. For both tasks, the FDB MTU length change is substantially larger than the fascicle length change (Step downs: MTU ~6 mm, Fascicles ~0.4 mm; Landings: MTU ~9 mm, Fascicles ~0.4 mm). The FDB MTU and fascicle velocities are shown in Figure 4D and E. We observed main effects for muscle level (MTU vs fascicle, $p < 0.001$) and task intensity (step down vs landings, $p < 0.001$), as well as an interaction effect ($p < 0.001$). Post hoc analyses revealed the interaction effect was driven by the increase in MTU lengthening velocity during the landings compared to the step-downs (Step downs: 54.7 ± 25.8 mm/s, Landing: 98.3 ± 43.2 mm/s; $p < 0.001$) and not by any changes in fascicle velocity between conditions (Step downs: 3.85 ± 3.31 mm/s, Landing: 6.05±5.49 mm/s; p = 0.234).

Muscle activation

The FDB EMG during the tasks is shown in figure 4C. The muscle is active prior to foot contact and remains active at a similar percentage of peak activation throughout the energy absorption phase for step downs (9-15% of max) and landings (12-18% of max). There were no statistically significant differences in mean (Step downs: 14.6 ± 10.59%, Landings: 17 ± 11.64%; $p = 0.413$) or peak (Step downs: 19.5 ± 14.31%, Landings: 21.4 ± 13.74%, $p = 0.644$) EMG between step-downs or landings.

Foot energetics

Peak power absorption (Step downs = -12.3 ± 12.7 W, Landings = -55.45 ± 40.6 W; $p = 0.002$) and negative work (Step downs = -6.9 ± 3.84 J, Landings = -14.9 ± 10.47 J; $p = 0.004$) at the foot was reduced during the step downs compared to the landings. During the step downs and landings, the peak in negative foot power following foot-ground impact occurs concurrently with the peak in MTU lengthening velocity (shown in figure 4F).

Discussion

Compression and recoil of the long arch in the foot allows energy storage and return via elastic stretch and recoil of the plantar aponeurosis, ligaments, and muscles that span this structure (Ker et al., 1987; Stearne et al., 2016; Kelly et al., 2019). In this study, we have shown that human long arch mobility can also be exploited during whole body accelerations and decelerations to add or remove mechanical

energy from the body. This is facilitated via a control scheme that decouples muscle fascicle and MTU lengthening behaviour, utilising energy storage in the tendinous tissues of the intrinsic foot muscles. When mechanical power output and input to the foot increased, the disparity between MTU and fascicle length changes and velocities increased, indicating greater utilisation of the tendinous tissues to amplify or buffer power output and inputs, with increasing demand. In addition to the known contribution of the passive elastic tissues within the arch of the foot (Ker, 1987; Stearne, 2016), this reveals an adaptive mechanism providing versatility for the foot to perform a myriad of locomotor tasks.

During the countermovement phase of the jump task, the MTU lengthened as the longitudinal arch compressed (lengthened and lowered), while the fascicles actively lengthened very slightly (~1mm), but generally remained quasi-isometric. This suggests that the FDB muscle is storing energy in the tendinous tissues during the countermovement, allowing force to be produced (and energy to be stored) over a longer period of time. Once MTU shortening had begun, both the MTU and fascicles shortened until toe-off in both tasks. Given that MTU shortening velocity was substantially faster than fascicle shortening velocity in the jumping condition, these data indicate the FDB muscle can utilize elastic energy during MTU recoil to generate power during propulsion. While the step up task did not require a countermovement, the same pattern of decoupling was evident in the early phase of the movement, with fascicles shortening for an extended period of time, prior to any length change occurring in the MTU. Previous research in the human gastrocnemius during jumping has demonstrated that similar MTU behaviour allows supramaximal power outputs, such that the stored elastic energy in the tendon adds to net energy generated by the fascicles and is returned at a faster rate than the fascicles could produce (Kurokawa et al., 2003; Farris et al., 2016). In our data, the period of MTU recoil coincided with a relatively large increase in foot power in jumping compared to the step ups, indicating the FDB fascicles utilize tendon elasticity to increase net power output from the MTU.

During the energy dissipation tasks the MTU length changes and velocities were an order of magnitude greater than those occurring in the muscle fascicles. When considered in context of the large magnitudes of energy dissipated at the foot during these tasks, this decoupling highlights the use of the tendinous tissues for energy absorption during the impact period. These findings for the FDB resemble the MTU dynamics of the lateral gastrocnemius of humans (Werkhausen et al., 2017) and wild turkeys (Konow et al., 2012; Konow and Roberts, 2015) during landing tasks. However, the decline in magnitude of GRF (force decay) sees this stored energy in gastrocnemius muscles returned to the muscles via tendon recoil while the fascicles actively lengthen, dissipating the energy stored in the tendon (Konow et al., 2012; Konow and Roberts, 2015; Werkhausen et al, 2017). Here, the FDB fascicles shortened during force decay with very little tendon recoil, perhaps indicating the energy remains stored in the tendon during subsequent weight bearing (and perhaps dissipated by the muscle when the foot is unloaded) or that the energy was dissipated elsewhere. However, an analysis over a

longer period of time would be necessary to resolve this. The large differences in MTU velocity relative to fascicle velocity in our data suggests that the FDB tendon acts as a buffer for the contractile tissues, sparing the muscle from experiencing high and potentially damaging strains and strain rates during rapid decelerations of the body (Konow et al., 2012; Konow and Roberts, 2015).

There is increasing evidence that the stiffness of the human foot is affected by more than the interaction between the longitudinal arch and the plantar fascia. Recently, the unique transverse curvature of the human foot has been revealed to play a part in the foot's stiffness (Venkadesan et al., 2020). The shape of the human foot is likely an important feature that enables considerable foot mobility, with the human midfoot actually displaying substantially more motion than that observed in non-human primates during locomotion (Holowka et al, 2017). We believe it is this unique osseous morphology combined with the muscle architecture and passive elastic tissues that enables such versatility in human foot function, as highlighted in a recent publication from our laboratory (Smith et. al. 2021). There is evidence for differences in foot muscle architecture across hominoids (Oishi, et al. 2009; Oishi et al., 2018), with fascicle lengths seemingly longer in gorillas, orangutans, chimpanzees, and bonobos. Longer fascicles (relative to muscle-tendon unit length) are better suited to generating joint excursion and power (Biewener, 2000; Roberts, 2011) and less suited to storage and return of elastic energy. As such, it is likely that, relative to those of other apes and hominids, the human foot is well adapted to utilize elastic energy from the intrinsic foot muscles, providing the versatility required for habitual upright locomotion. (Kelly, 2018; Riddick, 2019; Smith, 2021).

Our findings must be considered amidst the experimental limitations. All fascicle images were taken from the compartment of the FDB in line with the 2nd metatarsal. Therefore, our results may be over-extrapolating the behaviour of the FDB muscle's other three compartments. Additionally, despite their similarities in muscle and tendon length ratios and function, our findings for the FDB may not represent the behaviour of other intrinsic (or extrinsic) foot muscles. In order to enable the collection of high-quality muscle fascicle images, the ultrasound transducer was fixated underneath the arch of the foot such that slipping of the transducer in any direction was largely eliminated. It is possible that pressure from the transducer against the sole of the foot may have influenced the natural motion of the foot and possibly the activation of the muscle. However, our measurements were within-subject comparisons, so any compensations made due to probe pressure would be present for all tasks measured. The shoe worn by all participants to protect the transducer and foot introduced additional compliance underneath the foot, as well as the possibility of altering external moment arms at the foot and ankle joints. While we chose a stiff foam to minimize any compliance and damping effects, the shoe likely dissipated some mechanical energy, which would be included in our UD foot power calculations.

Variations in human feet morphology and innervation are known to exist between males and females, which could result in differences in foot function during locomotion. Thus, it was intended to recruit equal numbers of female and male participants. However, due to recruitment restraints imposed by

Covid-19, only a convenience sample was obtained and this sample did not have equal balance of male and female participants. Of note, the similarities of human feet between sexes far outweigh their differences, particularly in regard to the anatomy of the foot's muscles and tendons. Therefore, we are confident in the results and interpretations of data in this work, albeit that there may be some subtle differences due to sex, race or other attributes that we are not able to distinguish here due to the relatively small and homogenous sample size.

In conclusion, we have demonstrated that the FDB utilises its tendinous tissues to enhance power outputs during arch recoil when mechanical energy is produced at the foot, as well as to buffer power input into its muscles fascicles while the foot dissipates energy. This is the first *in vivo* evidence that the energy generation and dissipation capacities of the foot are modulated by the muscle and tendon dynamics of the intrinsic foot muscles and further highlights the importance of tendon compliance across human lower limb muscles for work generation and energy absorption.

Acknowledgements

We thank Max Andrews for his help in data collection.

Competing Interests

No competing interests declared.

Funding

This work was funded by an Australian Research Council Linkage Grant (LP160101316), in collaboration with Asics Oceania and The Australian Sports Commission.

Data Availability

A copy of the matfile and code to plot all dependent variable can be found at https://doi.org/10.48610/f3819a6.

List of Abbreviations

IFM-Intrinsic foot muscles

FDB-Flexor Digitorum Brevis

AH-Abductor Hallucis

MTU-Muscle-tendon unit

MTP-Metatarsalphalangeal

COM-Centre of mass

EMG-Muscle activation data

UD-Unified deformable

References

Biewener, A. A., & Roberts, T. J. (2000). Muscle and tendon contributions to force, work, and elastic energy savings: a comparative perspective. *Exerc. Sport Sci. Rev.*, 28(3), 99-107.

Cronin, N. J., Carty, C. P., Barrett, R. S., & Lichtwark, G. (2011). Automatic tracking of medial gastrocnemius fascicle length during human locomotion. *J. App. Physiol.*, 111(5), 1491-1496.

Dempster, W.T. (1955). *Space requirements of the seated operator: geometrical, kinematic, and mechanical aspects of the body with special reference to the limbs*. Ann Arbor, Michigan: University of Michigan.

Derrick, T. R., van den Bogert, A. J., Cereatti, A., Dumas, R., Fantozzi, S., & Leardini, A. (2020). ISB recommendations on the reporting of intersegmental forces and moments during human motion analysis. *J. Biomech.*, 99, 109533.

Farris, D. J., & Sawicki, G. S. (2012). The mechanics and energetics of human walking and running: a joint level perspective. *J. R. Soc. Interface*, 9(66), 110-118.

Farris, D. J., & Lichtwark, G. A. (2016). UltraTrack: Software for semi-automated tracking of muscle fascicles in sequences of B-mode ultrasound images. *Comput. Meth. Prog. Bio.*, 128, 111-118.

Farris, D. J., Lichtwark, G. A., Brown, N. A., & Cresswell, A. G. (2016). The role of human ankle plantar flexor muscle–tendon interaction and architecture in maximal vertical jumping examined in vivo. *J. Exp. Bio.*, 219(4), 528-534.

Farris, D. J., Kelly, L. A., Cresswell, A. G., & Lichtwark, G. A. (2019). The functional importance of human foot muscles for bipedal locomotion. *P. Natl. A. Sci. USA*, 116(5), 1645-1650.

Fukunaga, T., Kubo, K., Kawakami, Y., Fukashiro, S., Kanehisa, H., & Maganaris, C. N. (2001). In vivo behaviour of human muscle tendon during walking. *P. R. Soc. B. Biol. Sci.*, 268(1464), 229-233.

Hanavan, E. P. (1964). A mathematical model of the human body. *Aerospace Medical Research Laboratories*, 1–149.

Holowka, N. B., O'Neill, M. C., Thompson, N. E., & Demes, B. (2017). Chimpanzee and human midfoot motion during bipedal walking and the evolution of the longitudinal arch of the foot. *J. Hum. Evol.*, 104, 23-31.

Ker, R. F., Bennett, M. B., Bibby, S. R., Kester, R. C., & Alexander, R. M. (1987). The spring in the arch of the human foot. *Nature*, 325(6100), 147-149.

Kelly, L. A., Kuitunen, S., Racinais, S., & Cresswell, A. G. (2012). Recruitment of the plantar intrinsic foot muscles with increasing postural demand. *Clin. Biomech.*, 27(1), 46-51.

Kelly, L. A., Lichtwark, G., & Cresswell, A. G. (2015). Active regulation of longitudinal arch compression and recoil during walking and running. *J. R. Soc. Interface*, 12(102), 20141076.

Kelly, L. A., Cresswell, A. G., & Farris, D. J. (2018). The energetic behaviour of the human foot across a range of running speeds. *Sci. Rep.*, 8(1), 1-6.

Kelly, L. A., Farris, D. J., Cresswell, A. G., & Lichtwark, G. A. (2019). Intrinsic foot muscles contribute to elastic energy storage and return in the human foot. *J. App. Physiol.*, 126(1), 231-238.

Konow, N., Azizi, E., & Roberts, T. J. (2012). Muscle power attenuation by tendon during energy dissipation. *P. R. Soc. B. Biol. Sci.*, 279(1731), 1108-1113.

Konow, N. and Roberts, T. J. (2015). The series elastic shock absorber: Tendon elasticity modulates energy dissipation by muscle during burst deceleration. *P. R. Soc. B. Biol. Sci.*, 282(1804), 20142800.

Kura, H., Luo, Z. P., Kitaoka, H. B., & An, K. N. (1997). Quantitative analysis of the intrinsic muscles of the foot. *Anat. Rec.*, 249(1), 143-151.

Kurokawa, S., Fukunaga, T., Nagano, A., & Fukashiro, S. (2003). Interaction between fascicles and tendinous structures during counter movement jumping investigated in vivo. *J. App. Physiol.*, 95(6), 2306-2314.

Leardini, A., Benedetti, M. G., Berti, L., Bettinelli, D., Nativo, R., & Giannini, S. (2007). Rear-foot, mid-foot and fore-foot motion during the stance phase of gait. *Gait Posture*, 25(3), 453-462.

Ledoux, W. R., Hirsch, B. E., Church, T., & Caunin, M. (2001). Pennation angles of the intrinsic muscles of the foot. *J. Biomech.*, 34(3), 399-403.

Lichtwark, G. A., & Wilson, A. M. (2006). Interactions between the human gastrocnemius muscle and the Achilles tendon during incline, level and decline locomotion. *J. Exp. Bio.*, 209(21), 4379-4388.

Lichtwark, G. A., Bougoulias, K., & Wilson, A. M. (2007). Muscle fascicle and series elastic element length changes along the length of the human gastrocnemius during walking and running. *J. Biomech.*, 40(1), 157-164.

McDonald, K. A., Stearne, S. M., Alderson, J. A., North, I., Pires, N. J., & Rubenson, J. (2016). The role of arch compression and metatarsophalangeal joint dynamics in modulating plantar fascia strain in running. *PloS one*, 11(4), e0152602.

Oishi, M., Ogihara, N., Endo, H., Komiya, T., Kawada, S. I., Tomiyama, T., ... & Asari, M. (2009). Dimensions of the foot muscles in the lowland gorilla. *J. Vet. Med. Sci.*, 71(6), 821-824.

Oishi, M., Ogihara, N., Shimizu, D., Kikuchi, Y., Endo, H., Une, Y., ... & Ichihara, N. (2018). Multivariate analysis of variations in intrinsic foot musculature among hominoids. *J. Anat.*, 232(5), 812-823.

Roberts, T. J., & Azizi, E. (2011). Flexible mechanisms: the diverse roles of biological springs in vertebrate movement. *J. Exp. Bio.*, 214(3), 353-361.

Riddick, R., Farris, D. J., & Kelly, L. A. (2019). The foot is more than a spring: human foot muscles perform work to adapt to the energetic requirements of locomotion. *J. Roy. Soc. Interface*, 16(150), 20180680.

Smith, R. E., Lichtwark, G. A., & Kelly, L. A. (2021). The energetic function of the human foot and its muscles during accelerations and decelerations. *J. Exp. Bio.*, 224(13), jeb242263.

Stearne, S. M., McDonald, K. A., Alderson, J. A., North, I., Oxnard, C. E., & Rubenson, J. (2016). The foot's arch and the energetics of human locomotion. *Sci. Rep.*, 6(1), 1-10.

Takahashi, K. Z., Kepple, T. M., & Stanhope, S. J. (2012). A unified deformable (UD) segment model for quantifying total power of anatomical and prosthetic below-knee structures during stance in gait. *J. Biomech.*, 45(15), 2662-2667.

Takahashi, K. Z., Gross, M. T., Van Werkhoven, H., Piazza, S. J., & Sawicki, G. S. (2016). Adding stiffness to the foot modulates soleus force-velocity behaviour during human walking. *Sci. Rep.*, 6(1), 1-11.

Venkadesan, M., Yawar, A., Eng, C. M., Dias, M. A., Singh, D. K., Tommasini, S. M., ... & Mandre, S. (2020). Stiffness of the human foot and evolution of the transverse arch. *Nature*, 579(7797), 97-100.

Wade, L., Lichtwark, G., & Farris, D. J. (2018). Movement strategies for countermovement jumping are potentially influenced by elastic energy stored and released from tendons. *Sci. Rep.*, 8(1), 1-11.

Welte, L., Kelly, L. A., Kessler, S. E., Lieberman, D. E., D'Andrea, S. E., Lichtwark, G. A., & Rainbow, M. J. (2021). The extensibility of the plantar fascia influences the windlass mechanism during human running. *P. R. Soc. B.*, 288(1943), 20202095.

Werkhausen, A., Albracht, K., Cronin, N. J., Meier, R., Bojsen-Møller, J., & Seynnes, O. R. (2017). Modulation of muscle–tendon interaction in the human triceps surae during an energy dissipation task. *J. Exp. Bio.*, 220(22), 4141-4149.

Figures

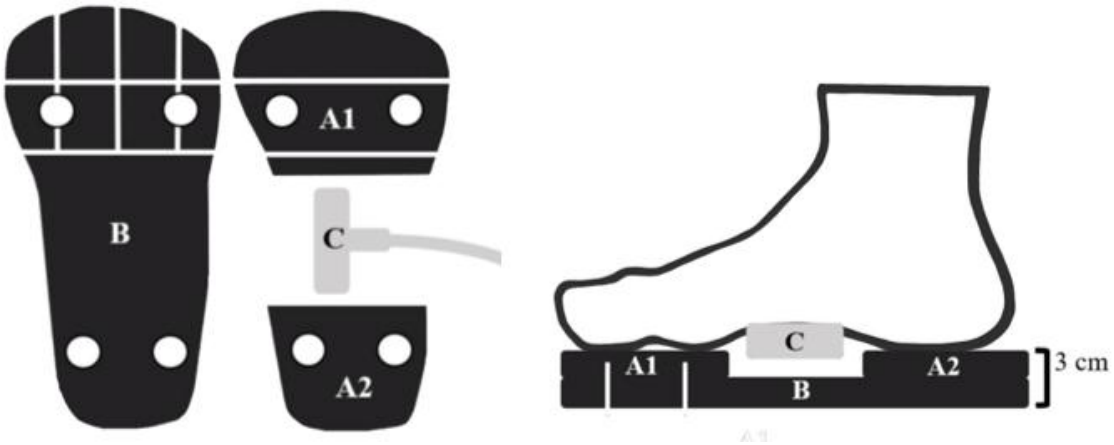

Figure 1. Foam shoe design to house the ultrasound probe during all experimental tasks, observed from the superior (left) and medial aspect (right). A cut-away in the midfoot region is used to house the probe. Three longitudinal and two transverse incisions are made in the foam to maximise the flexibility of the shoe and enable natural motion of the forefoot and toes during the experimental tasks. These incisions are depicted as white lines in each image.

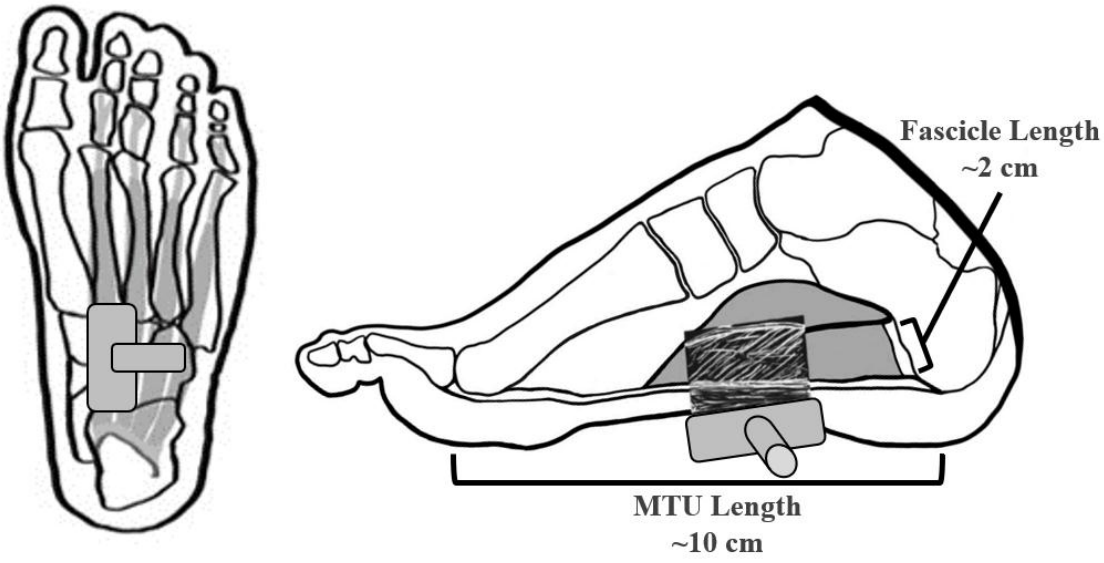

Figure 2. Orientation of the ultrasound transducer from inferior (left) and medial (right) aspects with depictions of the flexor digitorum brevis (shaded grey) and nearby foot anatomy. In the medial aspect, a typical example of an ultrasound image for the flexor digitorum brevis is depicted to aid in visualizing the muscle's architecture, and muscle and total muscle-tendon unit (MTU) lengths from Kura et al. (1997) and Ledoux et al. (2001) are provided.

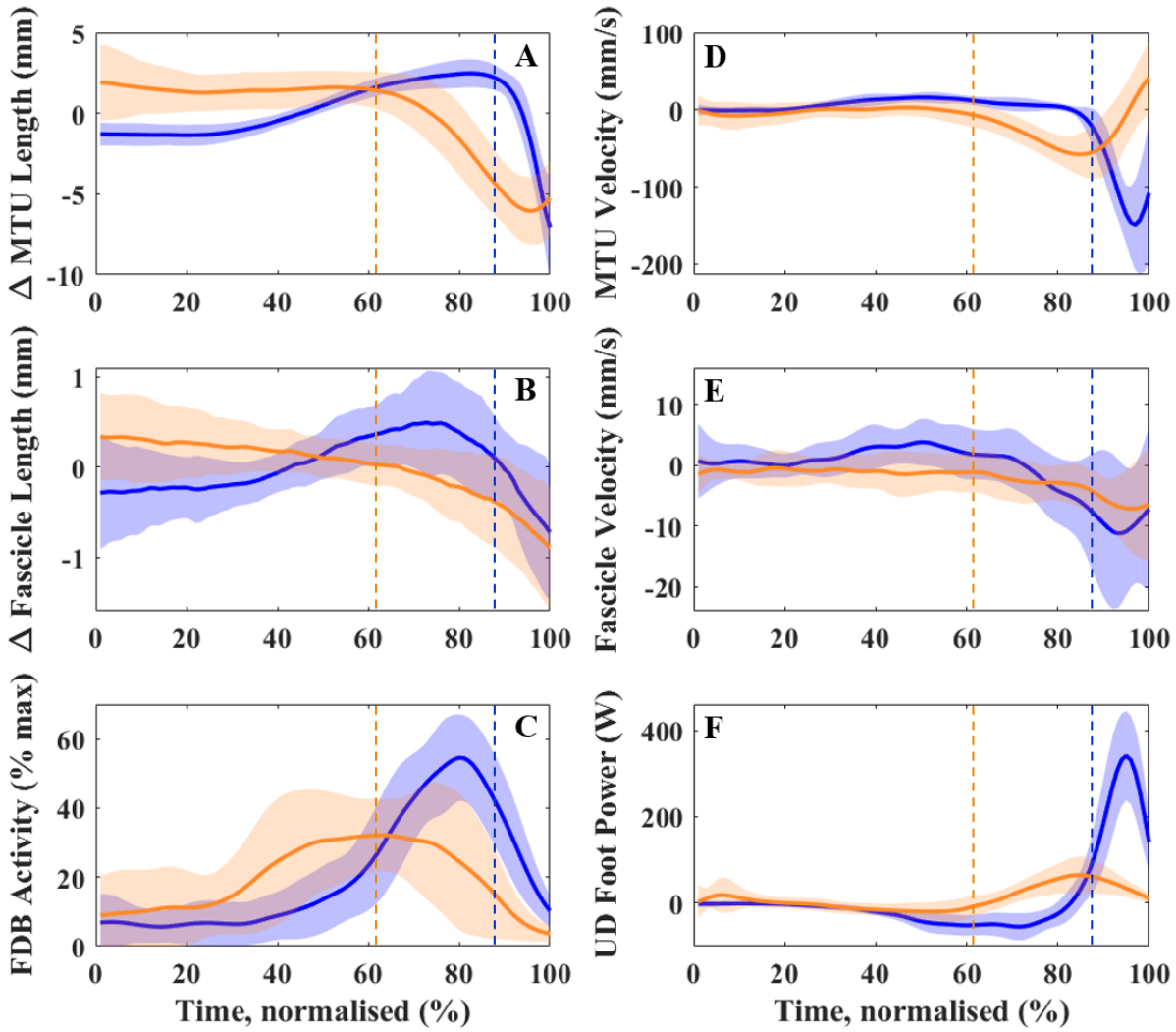

Figure 3. Group mean ensemble data obtained during the energy generation tasks for MTU length (A), fascicle length (B), FDB rectified muscle activity (C), MTU velocity (D), fascicle velocity (E), and UD foot power (F). Data from the step-ups (orange) and jumps (blue) are time normalised over the defined movement phases. Dotted vertical lines at 61% of normalised movement time (step-ups) and 89% of normalised movement time (jumps) represent the start of the FDB MTU shortening phase.

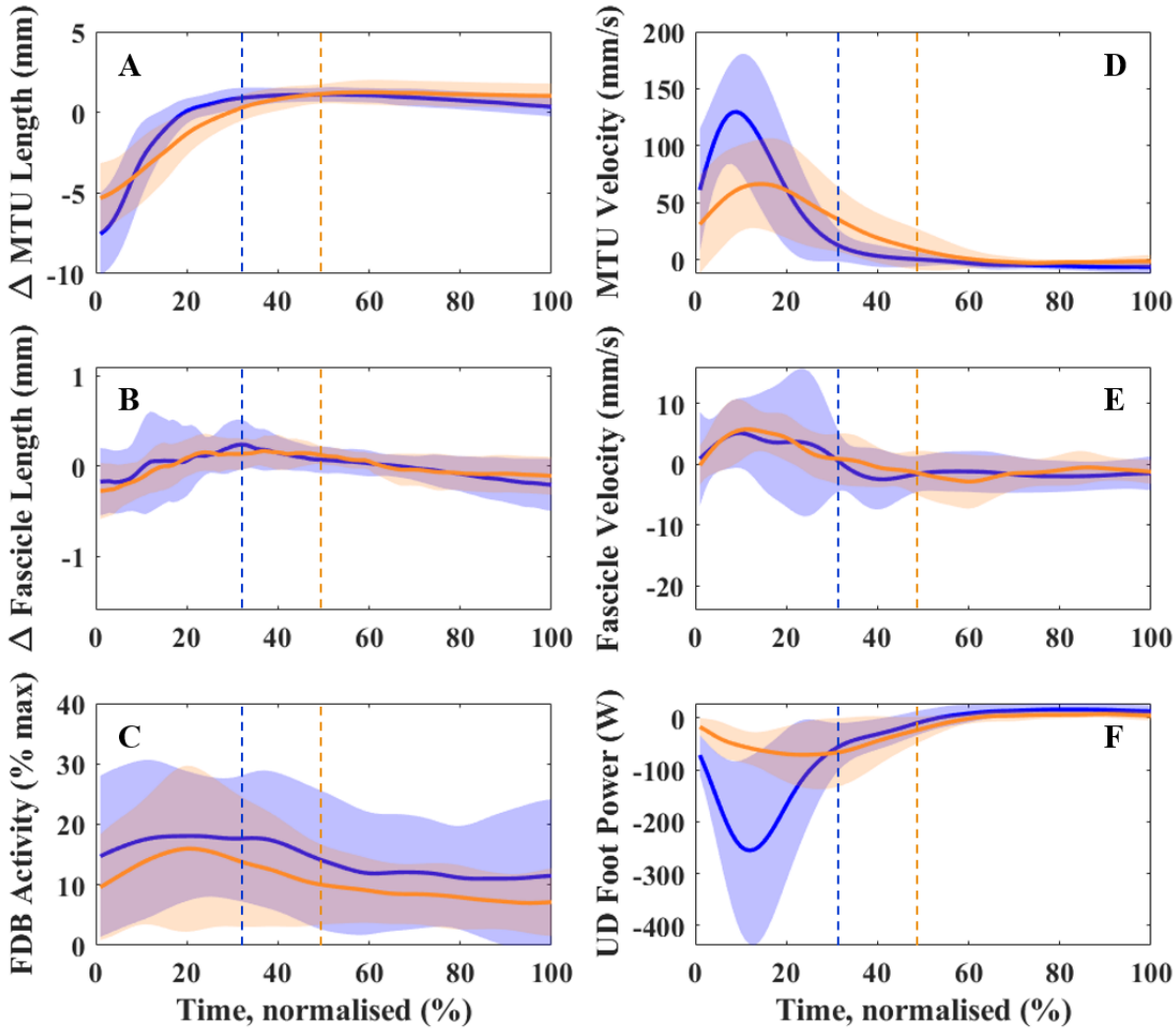

Figure 4. Group mean ensemble data obtained during the energy dissipation tasks for MTU length (A), fascicle length (B), FDB rectified muscle activity (C), MTU velocity (D), fascicle velocity (E), and UD foot power (F). Data from the step-downs (orange) and landings (blue) are time normalised over the defined movement phases. Dotted vertical lines at 48% of normalised time (step-downs) and 33% of normalised time (landings) represent the start of the FDB MTU lengthening phase.